Scaling variability from stellar to supermassive black holes

Done, Chris; Gierliski, Marek

Published in:
Monthly Notices of the Royal Astronomical Society

DOI:
10.1111/j.1365-2966.2005.09555.x

Publication date:
2005

Document Version
Publisher's PDF, also known as Version of record

Mon. Not. R. Astron. Soc. **364,** 208–216 (2005) doi:10.1111/j.1365-2966.2005.09555.x

Scaling variability from stellar to supermassive black holes

Chris Done[1] and Marek Gierliński[1,2]★

[1]*Department of Physics, University of Durham, South Road, Durham DH1 3LE*
[2]*Obserwatorium Astronomiczne Uniwersytetu Jagiellońskiego, 30-244 Kraków, Orla 171, Poland*

Accepted 2005 August 24. Received 2005 August 3; in original form 2005 May 10

ABSTRACT

We investigate the correspondence between the variability seen in the stellar and supermassive black holes. Galactic black hole (GBH) power density spectra (PDS) are generally complex, and dependent on spectral state. In the low/hard state the high-frequency rollover in the PDS moves in a way which is not simply related to luminosity. Hence this feature can only be used as an approximate indicator rather than as an accurate tracer of black hole mass in active galactic nuclei (AGNs). The X-ray spectrum in the high/soft state is dominated by the disc in the GBH, which is rather stable. We show that the PDS of the Comptonized tail in GBHs can be much more variable, and that it is this which should be compared to AGNs due to their much lower disc temperature. This bandpass effect removes a problem in interpreting the (often highly variable) narrow-line Seyfert 1 (NLS1) galaxies as the counterparts of the high mass accretion rate GBHs. Additionally, we speculate that some NLS1s (e.g. Akn 564) are counterparts of the very high state. The Comptonized tail in this state is also highly variable, but with PDS which can be roughly described as band-limited noise. This shape is similar to that seen in the low/hard state, so merely seeing such band-limited noise in the power spectrum of an AGN does not necessarily imply low luminosity. We also stress that Cygnus X-1, often used for comparison with AGNs, is not a typical black hole system due to its persistent nature. In particular, the shape of its power spectrum in the high/soft state is markedly different from that of other (transient) GBH systems in this state. The fact that the NLS1s NGC 4051 and MCG –6–30–15 do appear to show a power spectrum similar to that of the high/soft state of Cyg X-1 may lend observational support to theoretical speculation that the hydrogen ionization disc instability does not operate in AGNs.

Key words: accretion, accretion discs – X-rays: binaries – X-rays: galaxies.

1 INTRODUCTION

Black holes have no hair; they are the simplest celestial objects, fully characterized by their mass and spin. Scaling between supermassive and Galactic black hole (GBH) systems should theoretically be very simple. There should be a fundamental similarity between the accretion flow as a function of $L/L_{\rm Edd}$, with only a weak dependence on black hole mass. For example, standard optically thick accretion disc models predict that the spectrum should be dominated by a multitemperature blackbody component (Shakura & Sunyaev 1973), irrespective of the factor of 10^5–10^8 difference in mass. The only significant difference should be the energy at which the peak in the spectrum is observed (in EF_E representation, where F_E is energy flux per unit energy). At the Eddington luminosity this should be $\sim$1 keV in GBHs and $\sim$10 eV in active galactic nuclei (AGNs). The idea of a (mostly) mass-invariant accretion flow is also backed by observational evidence for simple scaling relations of the accretion flow between very different mass black holes (Merloni, Heinz & di Matteo 2003; Falcke, Körding & Markoff 2004).

However, observations also clearly show that the accretion flow is much more complicated than the simple Shakura–Sunyaev disc model. GBHs show a variety of different types of X-ray spectral and variability behaviour, which are used to classify the accretion flow into different spectral states (e.g. Tanaka & Lewin 1995; van der Klis 2000; Done & Gierliński 2003; Zdziarski & Gierliński 2004; McClintock & Remillard 2006). At high luminosity ($L/L_{\rm Edd} \gtrsim 0.2$) the GBHs show two main spectral states: the high/soft (or thermal dominant) and very high (steep power law). Both of these generally have peak energy output at $\sim$1 keV, as expected from an optically thick disc at these high mass accretion rates. However, they also show a tail of emission to higher energies produced by Compton scattering of seed photons from the disc by energetic electrons. This tail is rather complex (e.g. Gierliński et al. 1999), but can roughly be described by a power law. In the high/soft state, this tail is rather weak and has energy spectral index $\alpha \sim 1$ (where

★E-mail: Marek.Gierlinski@durham.ac.uk

$F_E \propto E^{-\alpha}$) while in the very high state, the tail carries a large fraction of the bolometric luminosity and has $\alpha \sim 1.5$. Conversely, at lower luminosities the GBHs can show qualitatively different emission, forming the low/hard state. Here they have only a weak disc component and have a dominant hard Comptonized tail. Again its shape is rather complex (e.g. the review by Zdziarski & Gierliński 2004), but can be roughly described as a power law of energy index $\alpha = 0.5$–1 (Tanaka & Lewin 1995; McClintock & Remillard 2006).

By analogy, the AGNs should also show these different X-ray spectral states (see, for example, White, Fabian & Mushotzky 1984 for an early example of this), and hopefully these intrinsic differences in spectra could explain some of the different types of AGN behaviour which cannot be modelled in simple orientation dependent unification schemes. In general, low-ionization nuclear emission-line regions (LINERs) have very low $L/L_{\rm Edd}$, so might correspond to the extreme (hardest spectra) low/hard states seen in GBHs, many Seyfert 1s are at a few per cent of Eddington, so could be bright low/hard state, while PG quasars and especially narrow-line Seyfert 1s (NLS1s) are generally at high $L/L_{\rm Edd}$, so would correspond to the high/soft or very high states of GBHs (Pounds, Done & Osborne 1995; see, for example, Boroson 2002; Woo & Urry 2002; Collin & Kawaguchi 2004 for estimates of $L/L_{\rm Edd}$). However, unlike the GBHs, transitions between these states are unobservable, making them more difficult to identify. The GBHs make transitions between the spectral states on time-scales of a few days (e.g. Cui et al. 1997; Wilson & Done 2001; Kalemci et al. 2004). This translates to time-scales of 300 to 3×10^5 yr when scaled from 10 $M_\odot$ to 10^6–10^9 $M_\odot$ black hole mass. The one exception is the very luminous system GRS 1915+105, where state transitions can occur on time-scales of a few seconds (Belloni et al. 2000), implying 10–1000 d time-scales in supermassive black holes.

None the less, AGNs do show substantial variability in their X-ray emission on time-scales of days and even hours (e.g. Nandra et al. 1997). Instead of true state transitions, this must correspond to the GBH variability seen on much shorter time-scales, between milliseconds and seconds. This range of time-scales is usually studied via power density spectra (PDS). In the GBHs, the PDS shape between 0.001 and 100 Hz is a strong function of the spectral state of the source, showing that the spectral and timing behaviours are generally correlated. For example, in Cygnus X-1, the overall shape of the PDS in the low/hard state can be approximately described as band-limited noise in νP_ν representation (where ν is frequency and P_ν is variability power at that frequency), with a 'flat top' ($P_\nu \propto \nu^{-1}$) so that most of the power is emitted between two break frequencies, $\nu_{\rm low} \sim 0.3$ Hz and $\nu_{\rm high} \sim 3$ Hz (e.g. Gilfanov, Churazov & Revnivtsev 1999). By contrast, its high/soft state has a high-frequency break at ∼14 Hz (e.g. Gilfanov et al. 1999) and no low-frequency break, so its overall shape is characteristic of a low-pass filter rather than of band-limited noise.

Here we look in more detail at the correspondence between AGN and GBH power spectra, as there are now a growing number of dedicated AGN monitoring campaigns. One of the goals of these studies is to use the characteristic time-scales in the PDS to estimate the black hole mass in AGNs. In particular, we stress that the high-frequency break is not constant, even within the low/hard state. So, while this break can be used as an indicator of black hole mass, it cannot be used to make accurate predictions. We also stress that at high mass accretion rates the GBH energy spectra are often dominated by the disc emission. This has very little variability compared to the Comptonized tail (Churazov, Gilfanov & Revnivtsev 2001), so it suppresses the rms variability in the high/soft state GBHs. The much lower disc temperature in AGNs means that their spectra are dominated by the Comptonized tail, so this bandpass effect means that AGNs can have much higher apparent rms variability. This removes one of the problems in identifying the often rapidly variable NLS1 galaxies (Leighly 1999) as the supermassive counterparts of the high/soft state (Pounds et al. 1995), while other issues due to the shape of the PDS can be resolved by recognizing the diversity of possible high mass accretion rate states. We caution that Cyg X-1 does not sample a large range in mass accretion rate, and shows a possibly unique PDS in its high/soft state. Thus, using this object as a template for AGN behaviour can severely distort attempts to scale the variability between supermassive and stellar black holes.

2 POWER SPECTRA OF GALACTIC BLACK HOLES

2.1 The data

We extract PDS of several GBHs corresponding to various spectral states in the (1/256)–128 Hz frequency band from the Proportional Counter Array (PCA) on board the *Rossi X-ray Timing Explorer* (*RXTE*). These PDS, shown in Fig. 1 in black, are calculated over the full energy band of the PCA (2–60 keV). We also extract high-energy power spectra, from ∼13–25 keV (starting at PCA channel 36 for Cyg X-1 and XTE J1550–564, and 26 for XTE J1650–500, and ending at channel 71 to avoid the background dominated energies), shown in Fig. 1 in light grey (cyan in colour). This high-energy band excludes most of the disc emission, so these PDS show the variability of the Comptonized tail alone.

We also extract both PCA and HEXTE energy spectra from the same observations using standard extraction and background subtraction criteria. These are shown in Fig. 2, where they are deconvolved from the instrument responses using the best-fitting model consisting of a multicolour accretion disc (DISKBB; Mitsuda et al. 1984), complex Comptonization (EQPAIR; Coppi 1999) and its reflection (Magdziarz & Zdziarski 1995; plus DISKLINE; Fabian et al. 1989). The total spectral model is also shown corrected for interstellar absorption. The power and energy spectra in Figs 1 and 2 were extracted from observations with the following archival numbers: a, 50110-01-38-01 ($L/L_{\rm Edd} = 0.011$); b, 60113-01-04-00 (0.049); c, 80135-01-02-00 (0.033); d, 10512-01-09-00 (0.063); e, 60113-01-19-00 (0.060); f, 30191-01-13-00 (0.25). All $L/L_{\rm Edd}$ values are calculated using bolometric luminosity estimated from the best-fitting model shown in Fig. 2. We used distances of 2 kpc (Herrero et al. 1995), 5.3 kpc (Orosz et al. 2002) and 4 kpc (Tomsick et al. 2003) and masses of 10 $M_\odot$ (Gierliński et al. 1999), 10 $M_\odot$ (Orosz et al. 2002) and 10 $M_\odot$ (Orosz et al. 2004) for Cyg X-1, XTE J1550–564 and XTE J1650–500, respectively.

2.2 Low/hard state

Cyg X-1 is often used as the 'canonical' GBH. Figs 1(a) and 2(a) show a typical power and energy spectrum from its low/hard state. The PCA energy spectrum is dominated by the hard Comptonized component, with little emission from the soft component visible in the data. The power spectra of the PCA data over the full- and high-energy bandpass are remarkably similar, with integrated fractional rms of 26.4 ± 0.2 and 24.8 ± 0.5 per cent, respectively, showing that the major variability on these time-scales is produced by the normalization of the tail varying, rather than its spectral shape. The typical low/hard state band-limited noise is evident in the PDS, with most of the power contained between ∼0.2 and 3 Hz so that the flat top spans an order of magnitude in frequency.

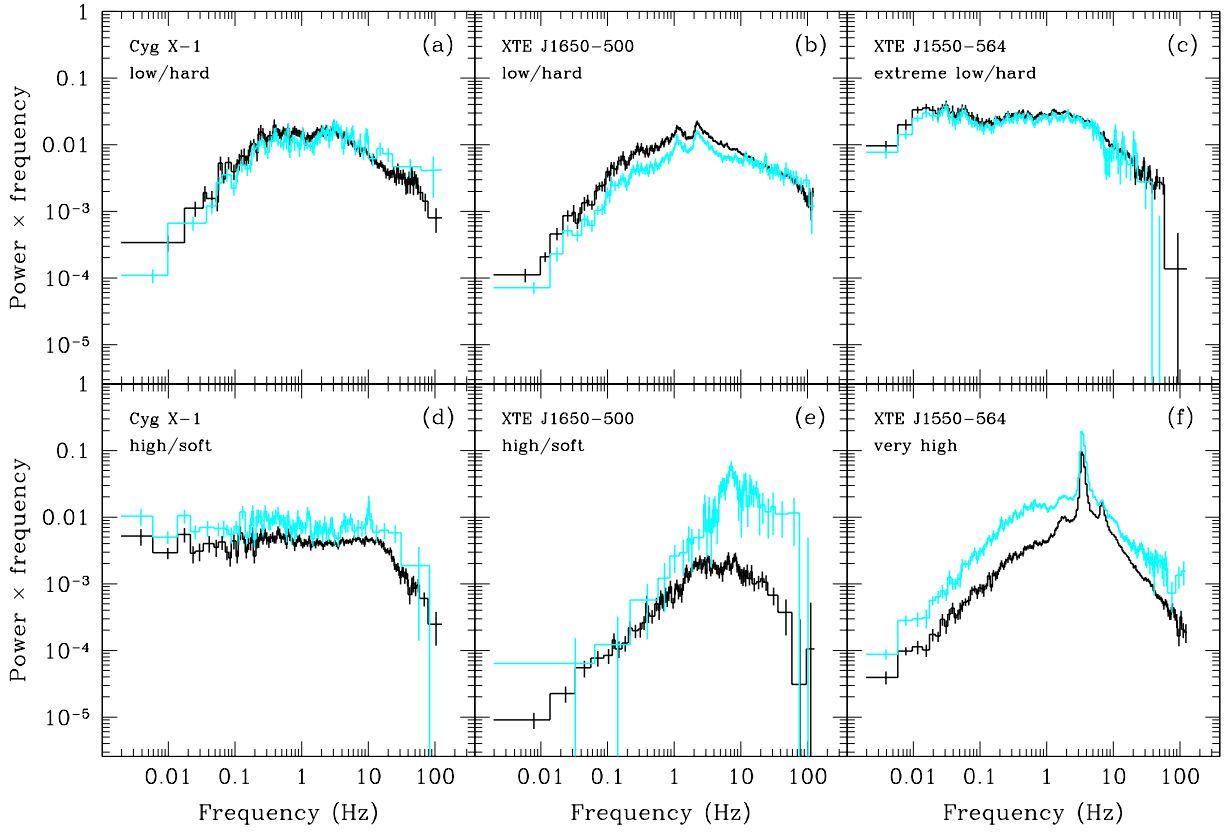

Figure 1. PDS from GBHs over the full (2–60 keV; black) and high-energy (∼13–25 keV; grey) bandpass of the PCA.

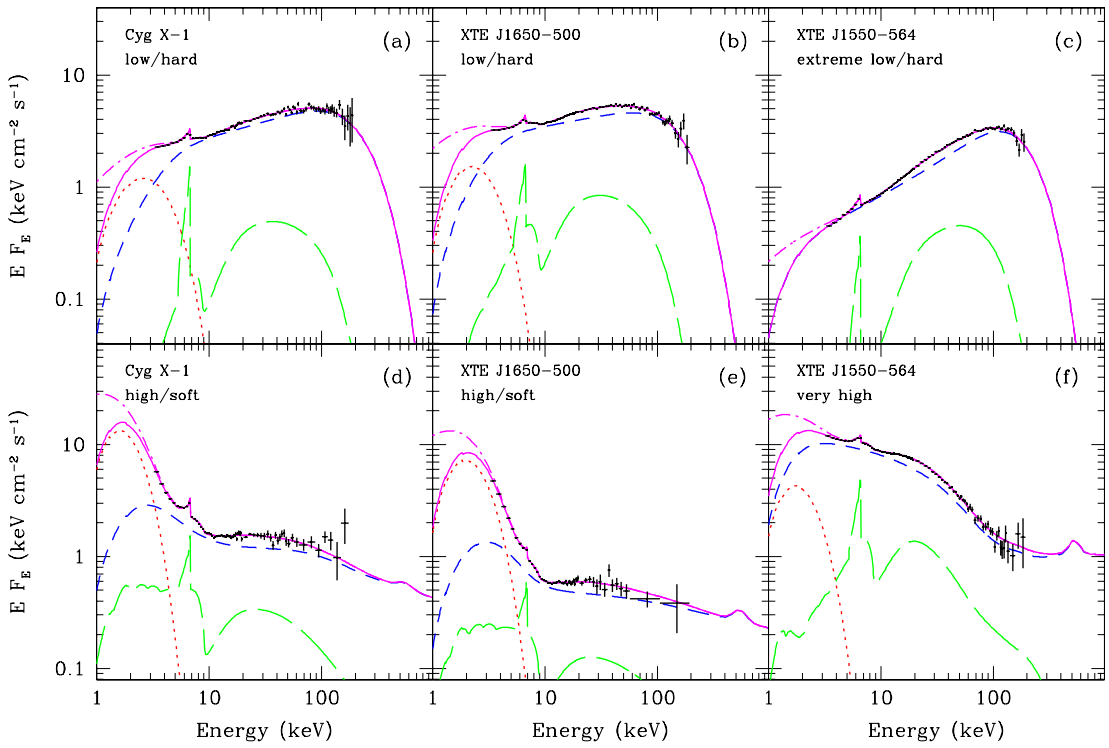

Figure 2. Unfolded energy spectra from PCA and HEXTE and best-fitting models corresponding to the each power spectrum shown in Fig. 1. The model components are plotted with different curves: the multicolour disc (dotted), complex Comptonization (dashed) and its reflection (long-dashed). The solid curve shows the sum. The dash-dotted curve represents unabsorbed total model.

As opposed to Cyg X-1, which is a persistent high-mass X-ray binary, the low-mass X-ray binary XTE J1650–500 is a transient source. Its low/hard state PDS is shown in Fig. 1(b), with corresponding energy spectrum in Fig. 2(b). These data were chosen so that the energy spectrum closely matched that of Cyg X-1 in Fig. 2(a). The power spectra are similar, but differ in detail. First, the shape of the power spectrum is less smooth – the band-limited noise is more clearly associated with quasi-periodic oscillation (QPO) components in XTE J1650–500 than in Cyg X-1. Secondly, the total rms is actually slightly decreased at higher energies, with 19.8 ± 0.1 per cent compared to 24.5 ± 0.1 in the full energy band, showing that the Comptonizing tail is pivoting with changing soft photon input (see Zdziarski et al. 2002 for similar behaviour in some 'failed transition' Cyg X-1 data).

Transient GBHs allow us to probe the behaviour of the power spectra over a much wider range of low/hard states than are sampled by Cyg X-1, which actually varies rather little in total bolometric power (e.g. Done & Gierliński 2003). Fig. 1(c) shows the power spectra of an extreme low/hard state from another transient, XTE J1550–564, where the (approximately) flat part of the power spectrum now extends over ∼2.5 orders of magnitude in frequency. The corresponding energy spectrum (Fig. 2c) shows that the Comptonized tail completely dominates the emission. The total rms variability of the power spectra is unchanged between the full PCA and high-energy PCA bandpasses, at 40.8 ± 0.4 and 39.8 ± 0.7 per cent, respectively, showing that the variability is dominated by simply the normalization of the tail, as in the Cyg X-1 low/hard data (Fig. 1a).

We can track the variation in these characteristic frequencies in the power spectrum throughout the low/hard state in this transient system. While multiple Lorentzian components are required to properly fit the PDS shape (Nowak 2000; Belloni, Psaltis & van der Klis 2002; Pottschmidt et al. 2003), the broad shape can be fairly well approximated by two Lorentzians (e.g. Axelsson, Borgonovo & Larsson 2005). We fitted the XTE J1550–564 power spectra from its 2000 and 2002 outbursts where the source was in the low/hard state by two Lorentzians, which gave a good description of the data. We also fitted the PCA/HEXTE broad-band energy spectra with a simple model consisting of the disc blackbody and thermal Comptonization (the model used by Done & Gierliński 2003) and used it to estimate the bolometric luminosity as a fraction of Eddington luminosity. The resulting peak frequencies of the two Lorentzians as a function of luminosity are shown in Fig. 3(a).

However, doubly broken power laws are generally used to fit AGN data. We would like to stress that generally these are not good descriptions of the GBH power spectra, where much better statistics reveals a more complex spectral shape. Nevertheless, we fitted the XTE J1550–564 power spectra by this model for comparison. We fixed the low-frequency PDS slope at zero, and the high-frequency slope at −2, and fitted for the low- and high-frequency breaks and the 'flat top' slope (which is generally close to unity), together with the overall normalization. We show the best-fitting break frequencies in Fig. 3(b). Although the break frequencies are different from the Lorentzian peak frequencies, the general behaviour from both models is similar: both frequencies move. This is more apparent for the low-frequency break, which can change by at least a factor of ∼50 between the outbursts, while the high-frequency break can change by at least a factor of ∼5 from the same object. There is a general correlation with $L/L_{\rm Edd}$ (Uttley et al. 2002) but this is *not* a one-to-one relationship, so the break frequency cannot be used as an accurate tracer of black hole mass.

We stress that these data are all taken from within the low/hard state, with energy spectral index $\alpha \sim 1.5$–1.6, and are not intermediate state or transition spectra. However, the behaviour seen in the 2000 outburst, where the low-frequency break moves by much more than the high-frequency break, continues into the hard-to-soft transition. This has the effect of decreasing the extent of the flat top and hence decreasing to the total rms (Gilfanov et al. 1999; Churazov et al. 2001; Pottschmidt et al. 2003; Axelsson et al. 2005). A very simple model for this correlated spectral and variability change is one in which a hot inner flow filters a spectrum of fluctuations from an outer cool disc. The inner and outer radii of the hot flow determine the high- and low-frequency breaks, respectively. As the disc moves inwards, the outer edge of the hot flow decreases, and $\nu_{\rm low}$ increases (Churazov et al. 2001), while the increasing disc flux for Compton scattering means that the spectrum becomes softer.

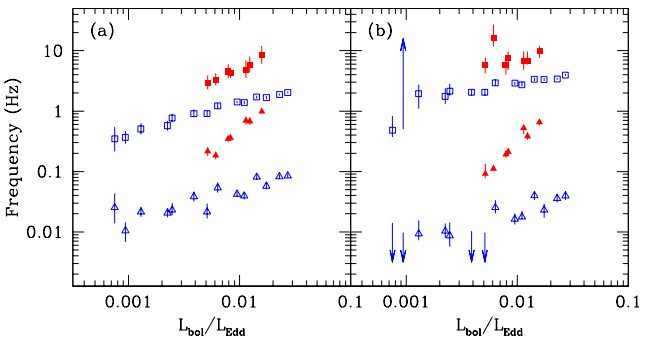

Figure 3. Characteristic frequencies in the hard-state PDS of the 2000 (filled symbols) and 2002 (open symbols) outbursts of XTE J1550–564. Triangles and squares correspond to lower and upper characteristic frequencies, respectively. (a) shows the peak frequencies of two Lorentzians, and (b) shows the break frequencies of the broken power law. In the 2000 outburst, the system reached the low/hard state from high/soft or very high state, and the pattern of PDS changes reflects those typically seen during the transition, in that the low-frequency break moves by much more than the high-frequency break. The 2002 outburst showed only low/hard state spectra, and here the low- and high-frequency breaks are consistent with changing together as the source dims.

2.3 High/soft state

Figs 1(d) and 2(d) show power and energy spectra of a typical Cyg X-1 high/soft state. The energy spectrum is now dominated by the disc component in the lowest PCA channels, but with a tail to higher energies. The disc emission is rather constant, while the tail is more variable (Churazov et al. 2001) so the contribution of the disc to the PCA spectrum will clearly suppress the rms variability observed. Fig. 1(d) shows that the total rms observed increases from 19.9 ± 0.5 to 27.3 ± 1.2 per cent when the power spectrum is made from the high-energy data alone, where there is negligible disc emission. The power spectral shape is also clearly very different to that seen in the low/hard state. Its shape is now similar to a low-pass filter, with only a single characteristic frequency which is the high-frequency rollover, $\nu_{\rm high} \sim 10$ Hz, while the flat top extends for over four decades in frequency.

Fig. 1(e) shows the power spectrum from equivalent high/soft state data from XTE J1650–500. These were chosen to closely match the energy spectrum to that seen from the Cyg X-1 high/soft data (Fig. 2e). Despite the strong energy spectral similarities, the power spectra are markedly different to that from the high/soft state in Cyg X-1 (Fig. 1d). The power spectrum of the high/soft state of XTE J1650–500 is strongly peaked. This matches smoothly on to the softest low/hard state power spectra described above, where the

flat part of the power spectrum shrinks to a very small frequency range. Cyg X-1 can also show such peaked power spectra (during its 'failed' transitions to the high/soft state; Pottschmidt et al. 2003), but its 'canonical' high/soft power spectrum seems dominated by a rather different power spectral component (see Fig. 1d, and also fig. 16 of Axelsson et al. 2005).

The spectrum of the high/soft state of XTE J1650–500 shows that the disc spectrum dominates the low-energy PCA bandpass, and so can strongly suppress the apparent variability. The Compton tail alone (high-energy PCA bandpass) has rms variability of 26.2 ± 1.8 per cent, whereas including the lower-energy, disc-dominated channels gives total variability of only 7.2 ± 0.2 per cent.

It is rather difficult accumulate enough signal-to-noise in the power spectra of the hard tail in the high/soft state of GBHs, especially when the disc has high temperature. Even if the tail is ∼10 per cent of the bolometric luminosity, its contribution to the total PCA count rate is much smaller for a high-temperature disc than for a lower-temperature one, due to the decreasing instrument response at higher energies. However, we have examined all the available high-energy power spectra from the outbursts of many GBHs and have never seen a high/soft state PDS which resembles that of the 'canonical' high/soft state derived from Cyg X-1. The high-energy power spectra are typically complex or strongly peaked, and show a variable rms from 5 to 30 per cent.

Thus, the Compton tail in the transient GBH shows a rather varied power spectrum in the high/soft state. It can be highly variable, with rms of ∼30 per cent, or it can be fairly constant (although still more variable than the disc) with rms of ∼5 per cent, but clearly there is no well-defined power spectral amplitude. However, where the tail has high rms variability, as seen in Cyg X-1, its shape is very different, showing strongly peaked noise which resembles QPO components rather than the smooth low-pass filter characteristic of Cyg X-1. The only transient GBHs to convincingly show a flat PDS extending over more than three orders of magnitude in frequency are those showing extreme low/hard energy spectra (Fig. 1c).

2.4 The very high state

Figs 1(f) and 2(f) show the power and energy spectra of the very high state of XTE J1550–564. The energy spectrum clearly has a disc component, but the Comptonized emission is also very strong, and dominates most of the PCA emission. The power spectral shape, especially at high energies, is similar to the low/hard state power spectra, i.e. band-limited noise, except that the QPO is much stronger and dominates the PDS (and makes the GBH PDS impossible to fit with the broken power-law model). The total rms for the full- and high-energy bandpass are 23.3 ± 0.1 and 32.3 ± 0.2 per cent, respectively. So, clearly again the variability is more marked by excluding the disc emission, but the effect is not so drastic as in the high/soft state, as the strong tail means the disc dilution is not so important. All very high state power spectra have high rms, and have this rather typical peaked noise shape, with strong QPOs.

Very high luminosities, even exceeding $L_{\rm Edd}$, can be seen from GRS 1915+105. While this source can show unique variability modes, probably connected with its uniquely high accretion rate (Done, Wardziński & Gierliński 2004), it spends about half of its time in a rather stable very high state (class χ; Belloni et al. 2000). PDS of these data show that they are very similar to those shown here for XTE J1550–564, with variability increasing at higher energies (Zdziarski et al. 2005).

3 APPLICATION TO ACTIVE GALACTIC NUCLEI

The GBH power and energy spectra shown in Figs 1 and 2 span the range of spectral states seen. However, they also illustrate the well-known lack of clean one-to-one correspondence between spectral state and luminosity (e.g. van der Klis 2001; McClintock & Remillard 2006) as all except the very high state are within a factor of a few from $L/L_{\rm Edd} \sim 0.03$. While, in general, the low/hard state is seen at $L/L_{\rm Edd} < 0.05$, it can extend up to ∼0.2 on the rapid rise to outburst. As we have yet to clearly understand the relation between GBH and AGN energy spectra, we use $L/L_{\rm Edd}$ as a guide to AGN spectral state. Those with $L/L_{\rm Edd} > 0.2$ are likely to correspond to high mass accretion rate GBHs, i.e. high/soft or very high state.

The much longer time-scales involved mean that only a few AGNs have been monitored to the extent that power spectra can be derived. The power spectra are also more complex to calculate than those from GBHs as the data are generally unevenly sampled. This gives a broad window function which redistributes power over a wide range of frequencies, so reconstructing the intrinsic power spectrum is analogous to deriving the intrinsic energy spectrum from the broad spectral response of an X-ray proportional counter. Techniques for this reconstruction generally rely on Monte Carlo simulations of the stochastic noise properties of a given power spectral form through the specific uneven sampling pattern corresponding to each AGN (Done et al. 1992; Uttley, McHardy & Papadakis 2002). These derived power spectra typically become less well defined at the lowest frequencies, so the uncertainties increase in the last decade in frequency of each reconstruction.

Table 1 gives basic data (black hole mass and Eddington fraction, which are uncertain by factors of at least 2–3) of a compilation of AGNs from the literature that have published power spectra; we reproduce the best-fitting models in Figs 4(a) and (b) for low and high mass accretion rates, respectively.

The different disc temperatures expected in AGNs and GBHs means that there is a bandpass effect which masks the expected similarities in the spectra and variability of the accretion flow. While the X-ray spectra of both AGNs and GBHs should be dominated by the hard Comptonized tail at low $L/L_{\rm Edd}$, the higher temperature disc expected in the GBHs means that this dominates their X-ray emission in the high/soft and very high states, while the corresponding AGN spectra will be dominated by the soft Comptonized tail seen in these states (see also McHardy et al. 2004). Thus, the AGN power spectra should be compared only to the high-energy power spectra in GBHs (cyan points in Fig. 1) not that derived from the total X-ray bandpass (black points).

However, there is also a secondary issue, which is the shape of the power spectrum. Cyg X-1 is not representative of the majority of the GBHs in terms of its power spectra, despite being used as the 'canonical' object. First, it is a persistent source, spanning very little range in bolometric luminosity, so it never shows a very high state, or an extreme low/hard state. Even over its limited observed range in $L/L_{\rm Edd}$, it generally has different power spectra to those of other (transient) GBHs with similar energy spectra. In its high/soft state, this is very marked, as the power spectra of the Compton tail has approximately equal power per decade between 10^{-3} and 10 Hz (probably extending down below 10^{-6} Hz; Reig, Papadakis & Kylafis 2002), giving a high rms of ∼30 per cent. By contrast, the transient GBHs with equivalent energy spectra show Compton tail power spectra that are often sharply peaked, or are complex, and have rms from 5 to 30 per cent. The low/hard state power spectrum

Table 1. A compilation showing estimated mass and $L/L_{\rm Edd}$ for the AGNs shown in Fig. 4 (i.e. those with published power spectra). The references are as follows: FH03, Filippenko & Ho (2003); MU05, Markowitz & Uttley (2005); M03, Markowitz et al. (2003); M04, McHardy et al. (2004); M05, McHardy et al. (2005); P02, Papadakis et al. (2002); P05, Peterson et al. 2005; R04, Romano et al. 2004; VF03, Vaughan & Fabian (2003); VFI04, Vaughan et al. (2004); V04, Vignali et al. (2004); WU02, Woo & Urry (2002). Ref.[1] refers to the mass and luminosity estimate, and Ref.[2] to the power spectrum shown in Fig. 4.

Source name	$\log M_{\rm BH}/{\rm M}_\odot$	Method	$L/L_{\rm Edd}$	Type	Ref.[1]	Ref.[2]
NGC 4258	7.62	Megamaser	0.005	LLAGN	WU02	MU05
Fairall 9	7.91	Reverberation	0.16	S1	WU02	M03
NGC 5548	8.03	Reverberation	0.05	S1	WU02	M03
NGC 4151	7.13	Reverberation	0.03	S1.5	WU02	M03
NGC 3516	7.36	Reverberation	0.06	S1	WU02	M03
NGC 4395	5.56(<4.81)	Reverberation(stellar velocity)	0.0012(>0.007)	S1	P05, FH03	VFI04
NGC 3783	6.94	Reverberation	0.23	S1	WU02	M03
Akn 564	6.9	Reverberation	0.96	NLS1	R04	V04, P02
MCG –6–30–15	6.71	Stellar velocity	0.40	NLS1	M05	M05
Mrk 766 (aka NGC 4253)	6.54	Optical luminosity	0.56	NLS1	WU02	VF03
NGC 4051	6.13	Reverberation	0.21	NLS1	WU02	M04

of Cyg X-1 is also subtly different from those seen in the transient systems, in that the QPO features are generally less marked.

3.1 Low $L/L_{\rm Edd}$ active galactic nuclei

A key goal of the AGN PDS studies is to use the high-frequency break as a tracer of black hole mass. Fig. 3 shows that the high-frequency break of a broken power-law description of the low/hard GBH PDS remains constant to within a factor of ∼5. So, while this cannot be used as an accurate tracer of black hole mass, it may give a zeroth-order indication.

The AGN shown in the left panel of Fig. 4 with $L/L_{\rm Edd} < 0.20$ could correspond to a variety of spectral states. Nonetheless, their PDS are consistent with being similar in both normalization and shape, and the majority of AGN on this plot (all with rather similar masses around $\sim 10^{7.5}\,{\rm M}_\odot$ and accretion rates of $L/L_{\rm Edd} \sim 0.1$: see Table 1), are compatible with scaling the high-frequency break from that seen in the bright low/hard state of Cyg X-1.

However, there are two clear exceptions to this, both of which are substantially lower $L/L_{\rm Edd}$ objects. NGC 4258 again has similar mass of around $\sim 10^{7.5}\,{\rm M}_\odot$, so its lower-frequency break could be due to it corresponding to a more extreme low/hard state (see Fig. 3). This is a clear counterexample to the idea of a universal PDS shape which depends only on mass (e.g Papadakis 2004; O'Neill et al. 2005), as indeed is shown by Fig. 3.

However, the lowest mass AGN known, NGC 4395, is not so easy to fit into this pattern. From the reverberation mass, it should have a high-frequency break only a factor of 100 higher than that from the other objects. Yet its break is ∼4–5 orders of magnitude higher than that for NGC 4258, the most obvious object to scale from in terms of similarly low $L/L_{\rm Edd}$, and ∼3 orders of magnitude from the majority of AGNs in the figure. Either there is truly a difference in the variability properties of AGNs and GBHs, or the black hole mass in NGC 4395 is overestimated. Some evidence for the latter possibility is that this is the only object which has significantly different masses inferred from reverberation and stellar velocity dispersion estimates (refs). Assuming instead that the mass is $\sim 10^4\,{\rm M}_\odot$, consistent with the stellar velocity upper limit, this gives $L/L_{\rm Edd} \sim 0.04$ and the PDS scales with mass in the same way as the majority of AGNs on the figure.

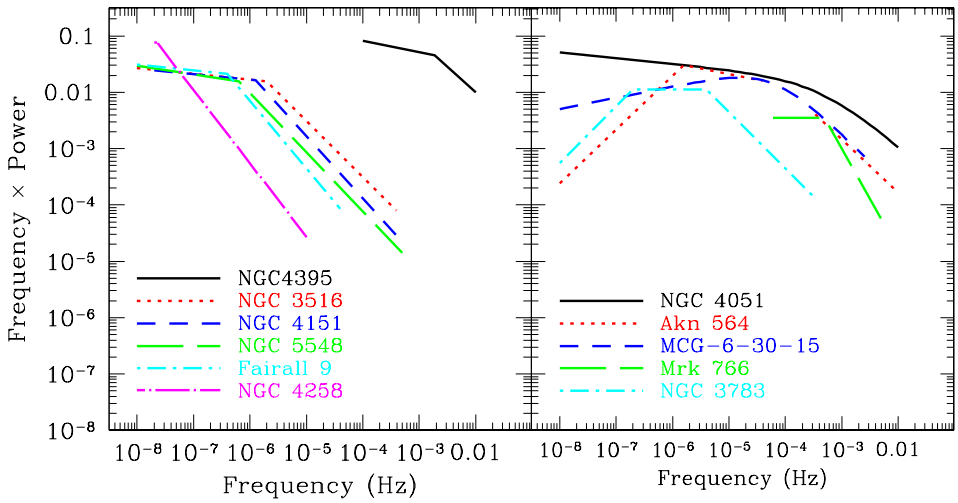

Figure 4. A compilation of derived model power density spectra from AGNs. (a) shows those for AGNs with inferred $L/L_{\rm Edd} < 0.2$, the approximate maximum seen for the low/hard state in GBHs. (b) shows those with $L/L_{\rm Edd} > 0.2$, so should correspond to high mass accretion rate (high/soft and very high state) GBHs. The PDS were taken from the literature listed in the last column of Table 1.

3.2 High $L/L_{\rm Edd}$ active galactic nuclei

By contrast, Fig. 4(b) shows those AGNs with $L/L_{\rm Edd} > 0.20$. Most of these have masses of $\sim 10^{6.5}$ $M_{\odot}$ but their PDS are very heterogeneous. This corresponds well with the multiple different types of PDS shape which can be seen in the high/soft and very high states from GBH.

Two of these AGNs (NGC 4051 and MCG–6–30–15, both NLS1s) clearly show flat noise power extending over more than four decades in frequency. These look very like that of the high/soft state in Cyg X-1, taking into account uncertainties in the low-frequency slope of the power spectra (McHardy et al. 2004, 2005). The total rms power in both is of the order of 25 per cent, again similar to that of the Comptonized tail in the high/soft state of Cyg X-1 (McHardy et al. 2004). Thus, these AGNs can be interpreted as the supermassive counterpart of the high/soft state Cyg X-1 data, which is not like the majority of transient GBH power spectra at high accretion rates.

However, another NLS1, Akn 564, convincingly shows band-limited flat top noise, where the flat top extends over only $\sim$ two decades in frequency (Fig. 4 taken from a combination of low- and high-frequency data in Markowitz et al. 2003 and Vignali et al. 2004). Such band-limited, high rms ($\sim$30 per cent) noise is consistent with the extreme low/hard state of GBHs (Fig. 1c). However, Akn 564 has high $L/L_{\rm Edd} \sim 1$ (Table 1), so should instead be comparable to the high mass accretion rate GBHs. Its PDS is clearly unlike that of NGC 4051 (and the high/soft state of Cyg X-1). Instead it could correspond to the PDS of the Compton tail seen in very high state (transient) GBHs (M$^{\rm c}$Hardy et al. 2004). These likewise show band-limited noise similar to that of the low/hard state, with the flat top extending over two decades in frequency, although this is usually accompanied by a strong QPO (Fig. 1f; Zdziarski et al. 2005). However, current AGN data probably cannot rule out the presence of even a very strong QPO such as that seen in the very high state because the uneven sampling strongly smears out the power (Vaughan & Uttley 2005). If a QPO is not present with better sampling of the AGN light curve, then it may be that Akn 564 instead represents a scaled-up version of a very high state from a persistent GBH. There are as yet no data on such GBH systems (Cyg X-1 never shows a very high state), but we speculate by analogy with the Cyg X-1 low/hard state PDS that these would have weaker QPO features than those seen in the transient systems.

Band-limited noise is also probably detected in another high $L/L_{\rm Edd}$ AGN, NGC 3783 (Markowitz et al. 2003). Here the situation is rather less clear, as $L/L_{\rm Edd} \sim 0.2$, i.e. close to the maximum low/hard state luminosity. Uncertainties in mass and bolometric luminosity mean this could easily fall or rise by a factor of 2–3. Thus, this could either represent a bright low/hard state or a dim very high state (sometimes termed an intermediate state; Belloni et al. 1996; Méndez & van der Klis 1997). These different 'states' merge smoothly together in the GBH, which can be explained in the context of a truncated disc extending closer to the black hole, increasing the overlap between the disc and hot inner flow as the source moves from low/hard to intermediate and very high states (Wilson & Done 2001; Kubota & Done 2004).

The only other high $L/L_{\rm Edd}$ AGN with published power spectrum is the NLS1, Mrk 766. Here there are no data on long time-scales, but the (evenly sampled) *XMM–Newton* data strongly indicate a break at $\sim 5 \times 10^{-4}$ Hz (Vaughan & Fabian 2003; Vaughan, Fabian & Iwasawa 2004). The normalization of the flat top noise is lower than that for the other AGNs (high or low $L/L_{\rm Edd}$), so this may correspond to a high state counterpart of a transient GBH.

4 HIGH/SOFT STATE OF CYG X-1 AND ITS IMPLICATIONS FOR ACTIVE GALACTIC NUCLEI

Despite its use as a template PDS, Cyg X-1's timing properties are not typical of GBHs. The high/soft state PDS is markedly different, with a flat top (in νP_{ν}) extending over at least four orders of magnitude in frequency. By contrast, power spectra of the Compton tail in other GBHs in the high/soft state are instead usually strongly peaked at $\sim$10 Hz, or have complex shapes.

The difference in Cyg X-1 is perhaps connected to the persistent nature of its emission due to the large accretion rate from its high-mass companion OB star. The X-ray bolometric luminosity varies by very little, $L/L_{\rm Edd} = 0.01$–0.1, over time-scales of weeks to years. By contrast, most GBHs have low-mass companions, with much lower mass transfer rates through the Roche lobe, and so have transient outbursts where the accretion flow luminosity changes from $L/L_{\rm Edd} \lesssim 10^{-7}$ to 0.05–1 (e.g. McClintock, Narayan & Rybicki 2004). We speculate that the large dynamic range of variability seen in transients may excite a rather different noise spectrum of turbulence in the disc. The observed PDS is the convolution of this intrinsic power spectrum with the response of the disc (e.g. Psaltis & Norman 2000). For a particular disc geometry, the response of the disc (its filter) is fixed (Psaltis & Norman 2000; Churazov et al. 2001), but if the intrinsic noise spectrum changes, then the observed PDS will also change.

It is currently unclear whether the disc instability which causes the dramatic outbursts in the transient GBH should also operate in AGNs, i.e. whether the initial spectrum of fluctuations is similar to that in Cyg X-1 or the transient GBH. The instability is triggered by the dramatic increase in opacity caused by the partial ionization of hydrogen at temperatures of $\sim 10^4$ K. Such temperatures are clearly expected in AGNs (Siemiginowska, Czerny & Kostyunin 1996; Burderi, King & Szuszkiewicz 1998). However, this needs to propagate globally through the disc rather than being a purely local instability in order to produce dramatic outbursts, which requires a change in the effective α viscosity parameter. This is probably produced in GBH discs by a change in viscosity mechanism, from the magneto-rotational instability (MRI) where hydrogen is ionized, to much weaker processes (e.g. spiral arms) where hydrogen is neutral. Physically, this could be linked to the large change in density of free electrons between the parts of the disc in which hydrogen is ionized and neutral. If the neutral disc is very neutral, then the lack of charge carriers suppresses the coupling of magnetic fields to the disc, shutting off the MRI viscosity (Gammie & Menou 1998). However, AGN discs at the critical hydrogen ionization temperature are much less dense than GBH discs at this temperature. Recombination processes, especially three-body recombination, will be much less efficient at these lower densities, so while hydrogen is mainly neutral there may be enough free electrons from potassium/iron, etc., to allow the MRI to still operate as a viscosity mechanism (Menou & Quataert 2001). Thus, the hydrogen ionization point would not trigger a global instability in AGN discs (Janiuk et al. 2004). However, this is still to some extent speculative, so it is not yet known whether we expect AGN variability to be more like persistent GBHs (i.e. Cyg X-1) or like the transients. The observation of a Cyg X-1 like high/soft power spectrum in the nearby NLS1, NGC 4051, argues for a suppression of the hydrogen ionization disc instability in this AGN, where the flat part of the power spectrum extends over more than four decades in frequency (McHardy et al. 2004). The lack of clear QPO signatures in AGNs (while mainly due to lack of statistics on the relevant time-scales; e.g. Vaughan 2005) may

also be a feature of a different disc turbulence spectrum characteristic of persistent sources. Better AGN power spectra, with better constraints on potential QPO signatures, could give observational insights into the operation of the MRI and hydrogen ionization instability in these massive discs.

5 CONCLUSIONS

Power spectra of AGNs are used to estimate the black hole mass by scaling characteristic time-scales (breaks) to those seen in the Galactic sources, most commonly using Cyg X-1 as the template PDS. However, this assumes that the PDS shape is constant, while the GBHs show clearly that the characteristic frequencies change significantly even within a single GBH state, and that the whole shape of the PDS can change with state transitions. However, this does not mean that scaling cannot yield useful constraints, although it certainly cannot give accurate black hole masses. The high-frequency break changes by only a factor of $\sim$5 within the low/hard state of GBHs, and this is rather less than the discrepancy inferred from relating break frequency to mass for the lowest mass known AGN, NGC 4395. Either the mass of this black hole is overestimated (for which there is some additional evidence), or there is some other variability process occurring which breaks the correspondence between this AGN and the GBH.

At high mass accretion rates, the X-ray spectra from GBHs can be dominated by the rather stable disc emission, while the much lower disc temperature in AGNs means that their X-ray spectra are dominated instead by the Compton tail. This bandpass effect means that the low variability, often cited as being characteristic of the high/soft state, is characteristic of the disc. At higher energies, where Comptonization dominates, GBHs can exhibit large amplitudes of variability, as required to match with AGNs, especially the NLS1s. The shape of the PDS in the high/soft state is generally strongly peaked, not at all like the low-pass filter PDS characteristic of the high/soft state in Cyg X-1. Because some NLS1s (NGC 4051 and MCG-6-30-15; McHardy et al. 2004, 2005) show PDS which look convincingly like Cyg X-1, we speculate that the hydrogen ionization instability (which gives rise to the transient behaviour in GBHs) does not operate in AGNs. However, there are also some NLS1s which show band-limited PDS, similar to those seen in the low/hard state. We show that such PDS can also be interpreted as transient high/soft state PDS or very high state PDS, so that band-limited noise is not a unique tracer of low mass accretion rates.

AGN variability can be interpreted as the supermassive analogue of the GBH variability, but only with careful matching of spectral states, and careful consideration of the different spectral components.

ACKNOWLEDGMENTS

We thank A. Markowitz, A. Siemiginowska and P. Uttley for enthusiastic discussions, and the anonymous referee for useful comments. MG acknowledges support through a UK Particle Physics and Astronomy Research Council (PPARC) Postdoctoral Research Fellowship (PDRF).

REFERENCES

Axelsson M., Borgonovo L., Larsson S., 2005, A&A, 438, 999
Belloni T., Mendez M., van der Klis M., Hasinger G., Lewin W. H. G., van Paradijs J., 1996, ApJ, 472, L107
Belloni T., Klein-Wolt M., Méndez M., van der Klis M., van Paradijs J., 2000, A&A, 355, 271
Belloni T., Psaltis D., van der Klis M., 2002, ApJ, 572, 392
Boroson T. A., 2002, ApJ, 565, 78
Burderi L., King A. R., Szuszkiewicz E., 1998, ApJ, 509, 85
Churazov E., Gilfanov M., Revnivtsev M., 2001, MNRAS, 321, 759
Collin S., Kawaguchi T., 2004, A&A, 426, 797
Coppi P. S., 1999, in Poutanen J., Svensson R., eds, ASP Conf. Ser. Vol., 161, High Energy Processes in Accreting Black Holes. Astron. Soc. Pac., San Francisco, p. 375
Cui W., Zhang S. N., Focke W., Swank J. H., 1997, ApJ, 484, 383
Done C., Gierliński M., 2003, MNRAS, 342, 1041
Done C., Madejski G. M., Mushotzky R. F., Turner T. J., Koyama K., Kunieda H., 1992, ApJ, 400, 138
Done C., Wardziński G., Gierliński M., 2004, MNRAS, 349, 393
Fabian A. C., Rees M. J., Stella L., White N. E., 1989, MNRAS, 238, 729
Falcke H., Körding E., Markoff S., 2004, A&A, 414, 895
Filippenko A. V., Ho L. C., 2003, ApJ, 588, L13
Gammie C. F., Menou K., 1998, ApJ, 492, L75
Gierliński M., Zdziarski A. A., Poutanen J., Coppi P. S., Ebisawa K., Johnson W. N., 1999, MNRAS, 309, 496
Gilfanov M., Churazov E., Revnivtsev M., 1999, A&A, 352, 182
Herrero A., Kudritzki R. P., Gabler R., Vilchez J. M., Gabler A., 1995, A&A, 297, 556
Janiuk A., Czerny B., Siemiginowska A., Szczerba R., 2004, ApJ, 602, 595
Kalemci E., Tomsick J. A., Rothschild R. E., Pottschmidt K., Kaaret P., 2004, ApJ, 603, 231
Kubota A., Done C., 2004, MNRAS, 353, 980
Leighly K. M., 1999, ApJS, 125, 297
McClintock J. E., Remillard R., 2006, in Lewin W. H. G., van der Klis M., eds, Compact Stellar X-ray Sources. Cambridge Univ. Press, Cambridge, in press
McClintock J. E., Narayan R., Rybicki G. B., 2004, ApJ, 615, 402
McHardy I. M., Papadakis I. E., Uttley P., Page M. J., Mason K. O., 2004, MNRAS, 348, 783
McHardy I. M., Gunn K. F., Uttley P., Goad M. R., 2005, MNRAS, 359, 1469
Magdziarz P., Zdziarski A., 1995, MNRAS, 273, 837
Markowitz A., Uttley P., 2005, ApJ, 625, L39
Markowitz A. et al., 2003, ApJ, 593, 96
Méndez M., van der Klis M., 1997, ApJ, 479, 926
Menou K., Quataert E., 2001, ApJ, 552, 204
Merloni A., Heinz S., di Matteo T., 2003, MNRAS, 345, 1057
Mitsuda K. et al., 1984, PASJ, 36, 741
Nandra K., George I. M., Mushotzky R. F., Turner T. J., Yaqoob T., 1997, ApJ, 476, 70
Nowak M. A., 2000, MNRAS, 318, 361
O'Neill P. M., Nandra K., Papadakis I. E., Turner T. J., 2005, MNRAS, 251
Orosz J. A. et al., 2002, ApJ, 568, 845
Orosz J. A., McClintock J. E., Remillard R. A., Corbel S., 2004, ApJ, 616, 376
Papadakis I. E., 2004, MNRAS, 348, 207
Papadakis I. E., Brinkmann W., Negoro H., Gliozzi M., 2002, A&A, 382, L1
Peterson B. M. et al., 2005, preprint (astro-ph/0506665)
Pottschmidt K. et al., 2003, A&A, 407, 1039
Pounds K. A., Done C., Osborne J. P., 1995, MNRAS, 277, L5
Psaltis D., Norman C., 2000, preprint (astro-ph/0001391)
Reig P., Papadakis I., Kylafis N. D., 2002, A&A, 383, 202
Romano P., 2004, ApJ, 602, 635
Shakura N. I., Sunyaev R. A., 1973, A&A, 24, 337
Siemiginowska A., Czerny B., Kostyunin V., 1996, ApJ, 458, 491
Tanaka Y., Lewin W. H. G., 1995, in Lewin W. H. G., van Paradijs J., van den Heuvel E., eds, X-Ray Binaries. Cambridge Univ. Press, Cambridge, p. 126
Tomsick J. A., Kalemci E., Corbel S., Kaaret P., 2003, ApJ, 592, 1100
Uttley P., McHardy I. M., Papadakis I. E., 2002, MNRAS, 332, 231
van der Klis M., 2000, ARA&A, 38, 717

van der Klis M., 2001, ApJ, 561, 943
Vaughan S., 2005, A&A, 431, 391
Vaughan S., Fabian A. C., 2003, MNRAS, 341, 496
Vaughan S., Uttley P., 2005, MNRAS, 362, 235
Vaughan S., Fabian A. C., Iwasawa K., 2004, preprint (astro-ph/0412695)
Vignali C., Brandt W. N., Boller T., Fabian A. C., Vaughan S., 2004, MNRAS, 347, 854
White N. E., Fabian A. C., Mushotzky R. F., 1984, A&A, 133, L9
Wilson C. D., Done C., 2001, MNRAS, 325, 167
Woo J.-H., Urry C. M., 2002, ApJ, 579, 530
Zdziarski A. A., Gierliński M., 2004, Prog. Theor. Phys. Suppl., 155, 99
Zdziarski A. A., Poutanen J., Paciesas W. S., Wen L., 2002, ApJ, 578, 357
Zdziarski A. A., Gierliński M., Rao A. R., Vadawale S. V., Mikolajewska J., 2005, MNRAS, 360, 825

This paper has been typeset from a TEX/LATEX file prepared by the author.